Optimization and Bayesian Inference in Model-based Decision Making

Ali Abdollahi
Major Advisor: Prof. Krishna R. Pattipati
Co-Advisor: Prof. Yaakov Bar-Shalom
Committee: Prof. K. R. Pattipati, Prof. Y. Bar-Shalom, Prof. S. Zhou

University of Connecticut
Department of Electrical and Computer Engineering

July 19, 2017

Outline

Publications

Book Chapter

1. **A. Abdollahi**, K. R. Pattipati, A. Kodali, S. Singh, S. Zhang, and P. B. Luh, "Probabilistic Graphical Models for Fault Diagnosis in Complex Systems," Part-I Ch. 5 in *Principles of Performance and Reliability Modeling and Evaluation*, Springer 2016. pp. 109–139.

Journal Papers

1. **A. Abdollahi**, X. Han, N. Raghunathan, B. Pattapati, B. Balasingam, K. R. Pattipati, Y. Bar-Shalom, and B. Card, "Optimal Charging for General Equivalent Electrical Battery Model, and Battery Life Management," *Journal of Energy Storage*, vol. 9, pp. 47–58, 2017.
2. **A. Abdollahi**, X. Han, G. V. Avvari, N. Raghunathan, B. Balasingam, K. R. Pattipati, and Y. Bar-Shalom, "Optimal battery charging, Part I: Minimizing time-to-charge, energy loss, and temperature rise for OCV-resistance battery model," *Journal of Power Sources*, vol. 303, pp. 388-398, 2016.

Conference Papers

1. **A. Abdollahi**, K. R. Pattipati, "Unification of Leaky Noisy OR and Logistic Regression Models and Maximum A Posteriori Inference for Multiple Fault Diagnosis Using the Unified Model," in *Proc., International Workshop on Principles of Diagnosis (DX)*, Denver, CO., Oct., 2016.
2. **A. Abdollahi**, N. Raghunathan, X. Han, G. V. Avvari, B. Balasingam, K. R. Pattipati, and Y. Bar-Shalom, "Battery charging optimization for OCV-resistance equivalent circuit model," in *Proc. American Control Conference (ACC)*, 2015, pp. 3467-3472.
3. **A. Abdollahi**, N. Raghunathan, X. Han, B. Pattipati, B. Balasingam, K. R. Pattipati, Y. Bar-Shalom, and B. Card, "Battery health degradation and optimal life management," in *Proc. IEEE AUTOTESTCON*, 2015, pp. 146-151.
4. B. Pattipati, B. Balasingam, **A. Abdollahi**, G. V. Avvari, K. R. Pattipati, and Y. Bar-Shalom, "Integrated battery fuel gauge and optimal charger," in *Proc. IEEE AUTOTESTCON*, 2014, pp. 260-269.

Other Publications with UCONN Affiliation:
(with primary authorship) 1 Journal Paper, 1 Conference Paper
(with co-authorship) 2 Journal Papers, 1 US Patent

Two-Level Charging Algorithm

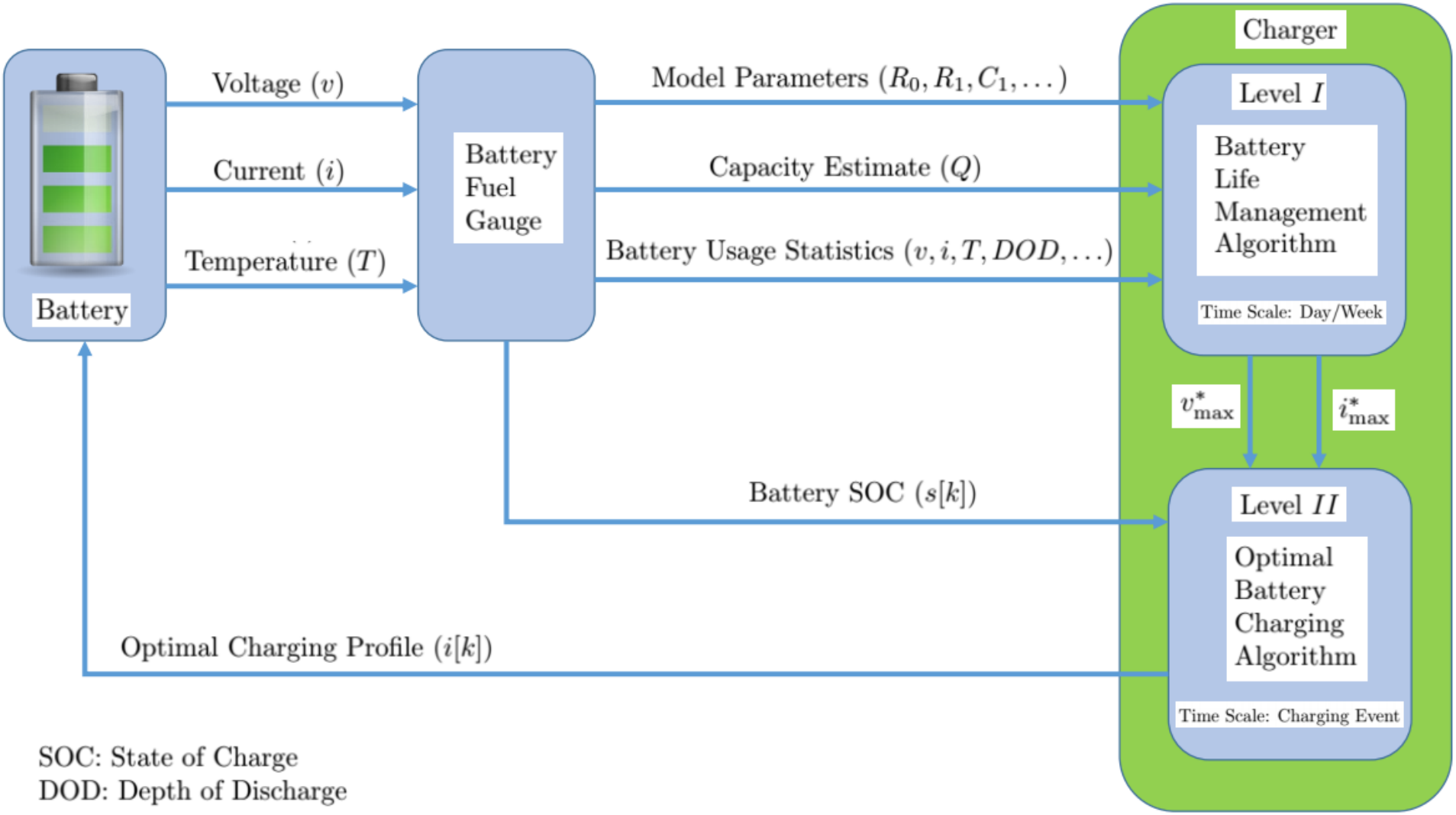

Figure 1: Battery management system (BMS) block diagram

Equivalent Electrical Circuit Battery Models

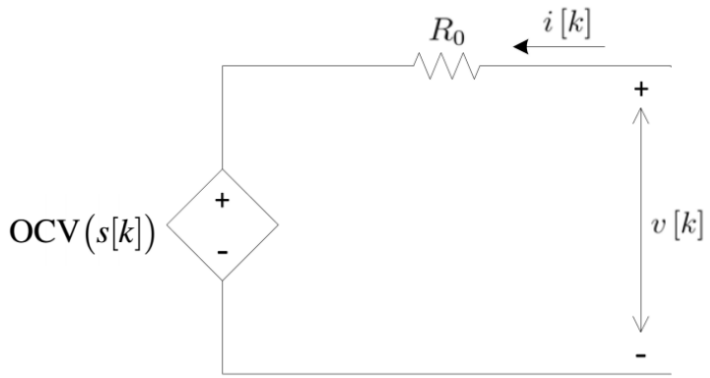

Figure 2: Equivalent electrical circuit model I of battery

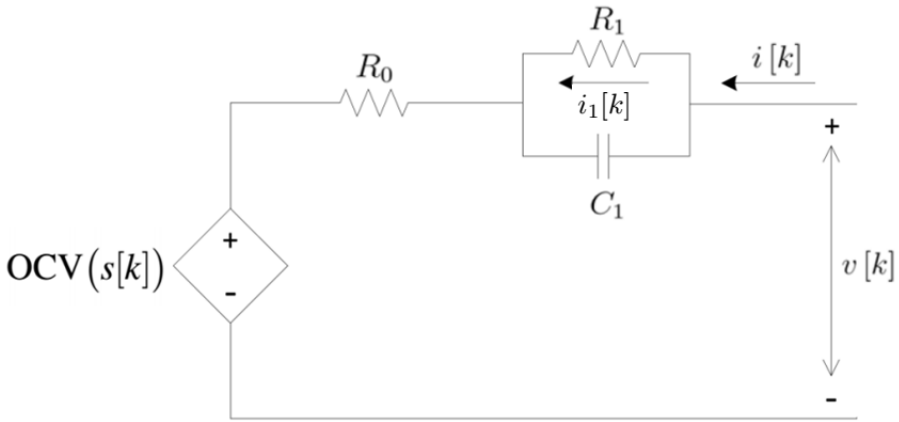

Figure 3: Equivalent electrical circuit model III of battery

In practice, equivalent electrical circuit models are used for batteries. These models normally include:

- An SOC-dependent Open-Circuit Voltage (OCV) Source
- A Resistance
- Possibly, one, two, or more parallel RC branches

The OCV is a nonlinear function of SOC:

$$z(s) \triangleq E + s(1-2E), \quad E = 0.15 \tag{1}$$

$$OCV(z) = K_0 + K_1 z^{-1} + K_2 z^{-2} + K_3 z^{-3} + K_4 z^{-4} + K_5 z + K_6 \ln(z) + K_7 \ln(1-z) \tag{2}$$

Typical OCV Curves

$SOC \in [0, 1]$

$SOC = 0$ indicates the battery is fully discharged.

$SOC = 1$ indicates the battery is fully charged.

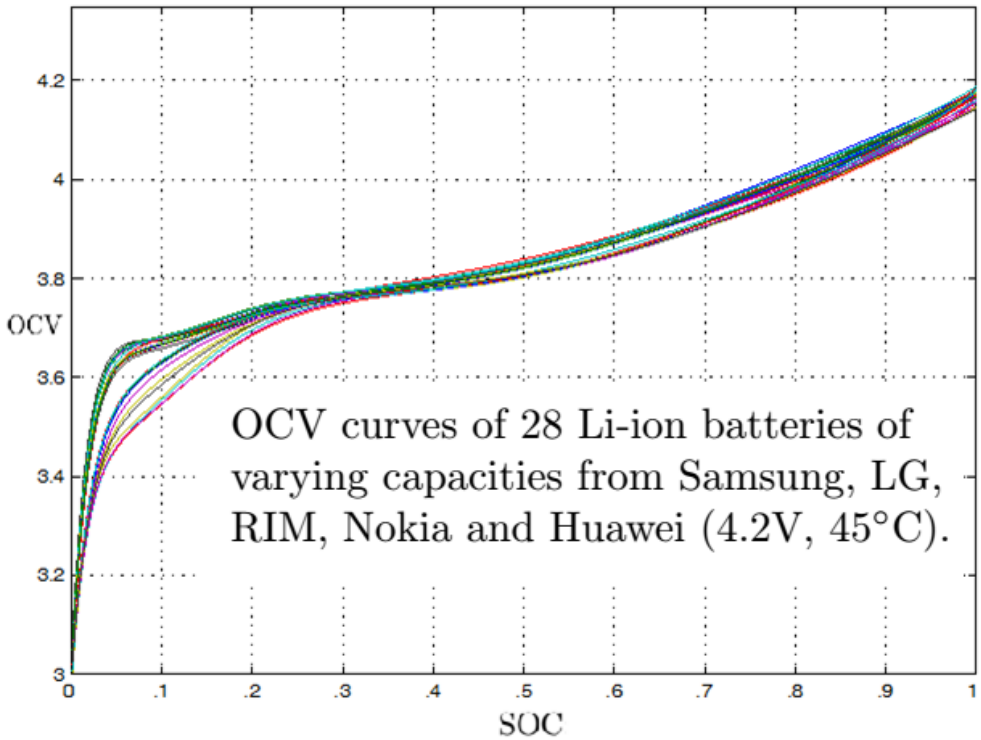

Figure 4: OCV curve as a function of SOC

Level II: Optimal Battery Charging for Model I

Initial SOC: $s[0] = s_0$
Final SOC: $s[k_f] = s_{k_f}$
SOC dynamics (Coulomb counting):

$$s[k+1] = s[k] + c_h i[k] \tag{3}$$

$$c_h = \frac{\Delta}{3600Q} \tag{4}$$

Δ: sampling time (in seconds)
Q: battery capacity (in Ah)

Constraint on battery terminal voltage:

$$\mathrm{OCV}\left(s[k]\right) + R_0 i[k] \leq v_c \tag{5}$$

Objective

Minimizing a weighted sum of time-to-charge (TTC) and energy loss (EL).

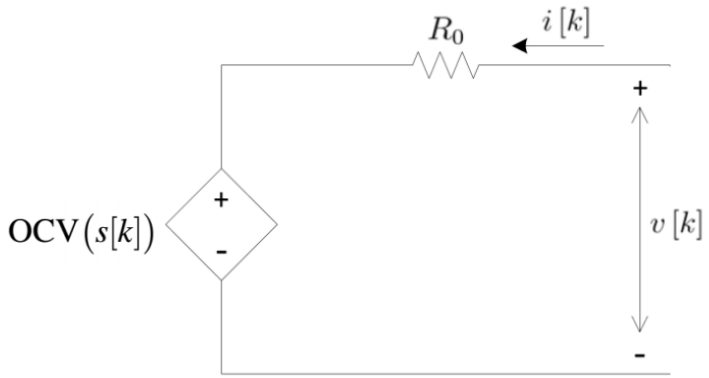

Figure 5: Equivalent electrical circuit model I of battery

Problem

Minimize

$$\rho_t J_t + J_E = \rho_t k_f \Delta + \sum_{k=0}^{k_f-1} R_0 i^2[k]\Delta \tag{6}$$

subject to:

$$s[k+1] = s[k] + c_h i[k] \quad s[0] = s_0 \quad s[k_f] = s_{k_f} \tag{7}$$

$$\mathrm{OCV}\left(s[k]\right) + R_0 i[k] \leq v_c \tag{8}$$

Minimization of Time and Energy Loss

Assume that at time k_1, the terminal voltage $v[k_1]$ reaches v_c and let $s[k_1] = s_1$.
Think of k_1 as the final time, and consider the problem of minimizing a "combination of time and energy loss". Δ is the sampling time.

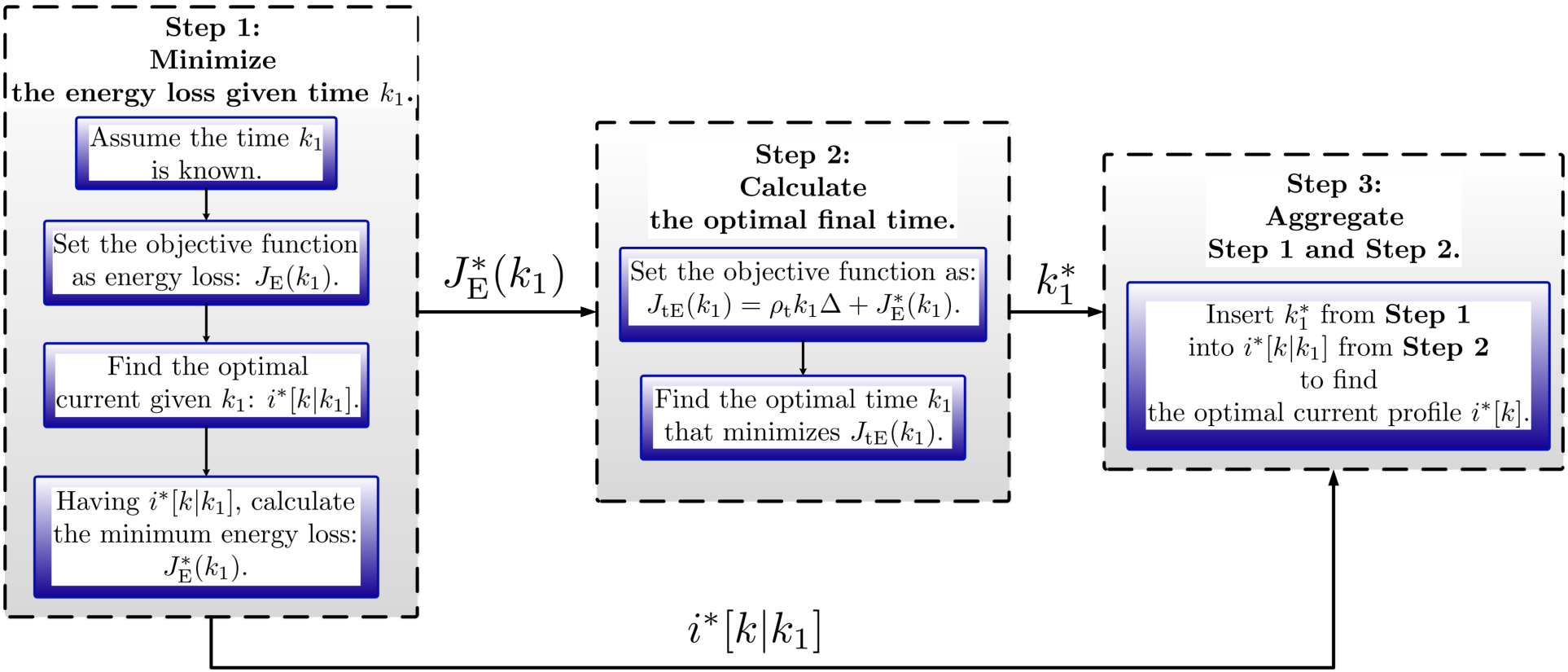

Figure 6: Minimization of time and energy loss

Deriving the Optimal Charging Profile for Model I

Step 1: Minimize the energy loss given time k_1

$$J_{\mathrm{E}}(k_1) = \sum_{k=0}^{k_1-1} R_0 i^2[k]\Delta \tag{9}$$

$$i^*[k|k_1] = \frac{s_1 - s_0}{k_1 c_h} \quad k = 0, 1, ..., k_1 - 1 \tag{10}$$

$$J^*_{\mathrm{E}}(k_1) = \frac{R_0\Delta(s_1 - s_0)^2}{k_1 c_h^2} \tag{11}$$

Step 2: Calculate the optimal final time

$$J_{\mathrm{tE}^*} = \rho_{\mathrm{t}} k_1 \Delta + \frac{R_0\Delta(s_1 - s_0)^2}{k_1 c_h^2} \tag{12}$$

$$k_1^* = \frac{s_1 - s_0}{c_h}\sqrt{\frac{R_0}{\rho_{\mathrm{t}}}} \tag{13}$$

Step 3: Aggregate Step 1 and Step 2

$$i^*[k] = \frac{s_1 - s_0}{k_1^* c_h} = \sqrt{\frac{\rho_{\mathrm{t}}}{R_0}} \quad k = 0, 1, ..., k_1^* - 1 \tag{14}$$

OtE Strategy

OtE Strategy: Optimal Solution for Time and Energy Loss Minimization

Constant-Current (CC) stage: $i[k] = \sqrt{\frac{\rho_t}{R_0}}$, while $v[k] < v_c$ Constant-Voltage (CV) stage: $v[k] = v_c$

To the best of our knowledge, this is the first time that it is proved that the well-known CC-CV charging profile is the optimal solution of a particular optimization problem, namely, the problem of minimizing the weighted sum of time-to-charge and energy loss for the OCV-Resistance model.

Animation 1: Effect of ρ_t

Animation 2: Effect of battery aging

Temperature Effects

Temperature model (linear part of the heat transfer equation):

$$\tilde{T}[k+1] = (1-a)\tilde{T}[k] + bi^2[k], \qquad \tilde{T}[0] = 0 \tag{15}$$

where, $\tilde{T}[k] = T[k] - T_{\text{amb}}$. The cost function including TTC, EL and temperature rise index (TRI) can be written as

$$J_{\text{tET}} = \rho_{\text{t}} J_{\text{t}} + J_{\text{E}} + \rho_{\text{T}} J_{\text{T}}, \quad J_{\text{T}} = \Delta \sum_{k=0}^{k_f} \tilde{T}[k] \tag{16}$$

We refer to the solution of (16) as OtET (Optimal time, Energy loss, Temperature). We can put the cost function J_{tET} in the following form:

$$J_{\text{tET}} = \rho_{\text{t}} k_f \Delta + \Delta \sum_{k=0}^{k_f-1} R_{\text{eq}}[k] i^2[k] \tag{17}$$

where $R_{\text{eq}}[k]$ is a time-dependent function of R_0 and the temperature model parameters.
In OtET the current profile in the first stage ($v[k] < v_c$) is as follows:

$$i^*[k] = -G_{\text{eq}}[k]\,(s_1 - s_0)/\big(c_h \sum_{k=0}^{k_1-1} G_{\text{eq}}[k]\big) \quad k = 0, 1, ..., k_1 - 1 \tag{18}$$

where $G_{\text{eq}}[k] = 1/R_{\text{eq}}[k]$. OtET can be approximated (referred to as Near-Optimal tET (NOtET)) as follows:

$$i^*[k] \approx \sqrt{\rho_{\text{t}}/\big(R_0(1+\rho_{\text{T}} R_{\text{Eff}})\big)} \quad k = 0, 1, ..., k_1 - 1 \tag{19}$$

where R_{Eff} is the effective thermal resistance (in kelvin/watt).

Effect of Temperature Rise Index (TRI)

As seen in Fig. 8, by including the TRI term, the battery temperature rises less.

Note that NOtET is a very good approximation to OtET.

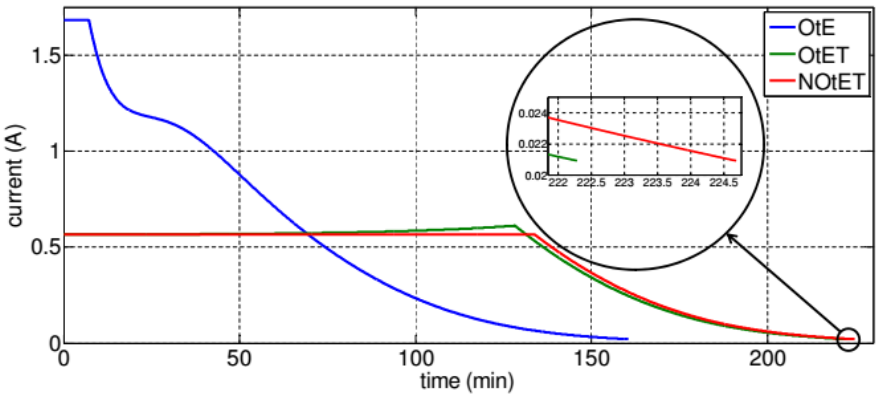

Figure 7: Current profiles for $\rho_t = 1$, $\rho_T = 1$

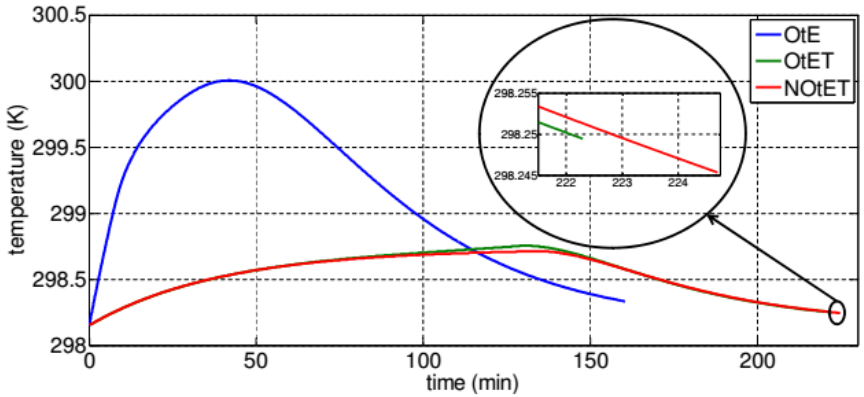

Figure 8: Temperature profiles for $\rho_t = 1$, $\rho_T = 1$

Level II: Optimal Battery Charging for Model III

SOC dynamics (Coulomb counting):

$$s[k+1] = s[k] + c_h i[k] \tag{20}$$

Dynamics of the current passing through R_1:

$$i_1[k+1] = \alpha i_1[k] + (1-\alpha) i[k] \tag{21}$$

$$\alpha = \exp(-\frac{\Delta}{R_1 C_1}) \tag{22}$$

Constraint on battery terminal voltage:

$$\mathrm{OCV}\,(s[k]) + R_0 i[k] + R_1 i_1[k] \leq v_c \tag{23}$$

Cost function:

$$J_{\mathrm{tEsT}} = \rho_{\mathrm{t}} J_{\mathrm{t}} + J_{\mathrm{E}} + \rho_{\mathrm{s}} J_{\mathrm{s}} + \rho_{\mathrm{T}} J_{\mathrm{T}} \tag{24}$$

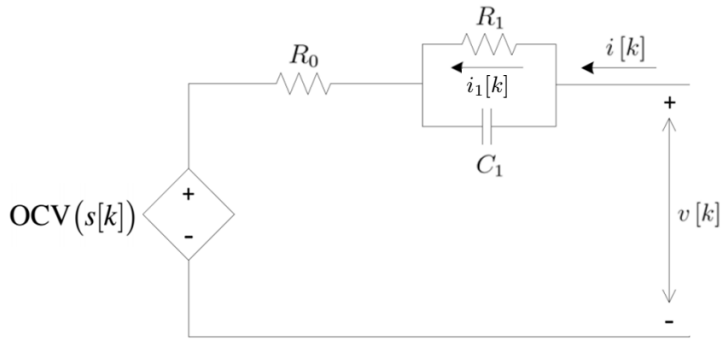

Figure 9: Equivalent electrical circuit model III of battery

$$J_{\mathrm{t}} = k_f \Delta \tag{25}$$

$$J_{\mathrm{E}} = \Delta \sum_{k=0}^{k_f-1} (R_0 i^2[k] + R_1 i_1^2[k]) \tag{26}$$

$$J_{\mathrm{s}} = \sum_{k=0}^{k_f-1} (s[k] - s_{k_f})^2 \tag{27}$$

$$J_{\mathrm{T}} = \Delta \sum_{k=0}^{k_f} \tilde{T}[k] \tag{28}$$

Level II: Optimal Battery Charging for Model III

$$\underline{z}[k] = \begin{bmatrix} s[k] - s_{k_f} \\ i_1[k] \end{bmatrix} \tag{29}$$

The dynamics of $\underline{z}[k]$ with its initial and final states could be written as follows:

$$\underline{z}[k+1] = \Phi \underline{z}[k] + \Gamma i[k] \tag{30}$$

$$\Phi = \begin{bmatrix} 1 & 0 \\ 0 & \alpha \end{bmatrix} \tag{31}$$

$$\Gamma = \left[c_h, 1-\alpha\right]^T \tag{32}$$

$$\underline{z}[0] = \left[s_0 - s_{k_f}, 0\right]^T \tag{33}$$

$$\underline{z}[k_f] = \left[0, \text{free}\right]^T \tag{34}$$

The battery terminal voltage is then as follows:

$$v[k] = \text{OCV}\left(s[k]\right) + R_0 i[k] + \begin{bmatrix} 0 & R_1 \end{bmatrix} \underline{z}[k] \tag{35}$$

Level II: Optimal Battery Charging for Model III

Solution

For a given k_1 value, the optimal current profile in stage 1 (the LQ stage) is obtained as follows:

$$i[k] = -\frac{\Gamma^T}{2\Delta R_{0\text{eq}}[k]}\left(P[k+1]\left((I_3+\Psi[k]P[k+1])^{-1}\left(\Phi \underline{z}[k]-\Psi[k]\underline{g}[k+1]\nu\right)\right)+\underline{g}[k+1]\nu\right) \tag{36}$$

where ν and $\Psi[k]$ are given by:

$$\nu = \frac{s_1 - s_{k_f} - \underline{g}^T[0]\underline{z}[0]}{\omega[0]} \tag{37}$$

$$\Psi[k] = \frac{\Gamma\Gamma^T}{2\Delta R_{0\text{eq}}[k]} \tag{38}$$

$\underline{z}[0]$ is the initial state.

$\underline{g}[0]$ and $\omega[0]$ are calculated by solving the following backward set of recursions:

$$\begin{aligned} P[k] &= 2\tilde{Q}[k] + \Phi^T P[k+1]\left(I_3+\Psi[k]P[k+1]\right)^{-1}\Phi \\ \underline{g}[k] &= \Phi^T\left(I_3+P[k+1]\Psi[k]\right)^{-1}\underline{g}[k+1] \\ \omega[k] &= \omega[k+1] - \underline{g}^T[k+1]\left(I_3+\Psi[k]P[k+1]\right)^{-1}\Psi[k]\underline{g}[k+1] \end{aligned} \tag{39}$$

$$\tilde{Q}[k] = \text{diag}\left(\rho_s,\ \Delta R_{1\text{eq}}[k]\right) \tag{40}$$

with the following terminal values:

$$P[k_1] = \begin{bmatrix} 0 & 0 \\ 0 & 0 \end{bmatrix},\ \underline{g}[k_1] = \begin{bmatrix} 1 & 0 \end{bmatrix}^T,\ \omega[k_1] = 0 \tag{41}$$

Effects of Different Weights for Model III

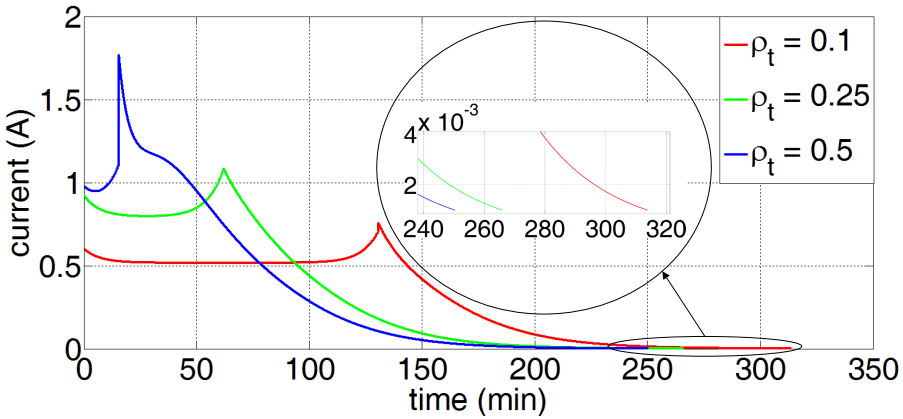

Figure 10: Current profiles for different values of ρ_t

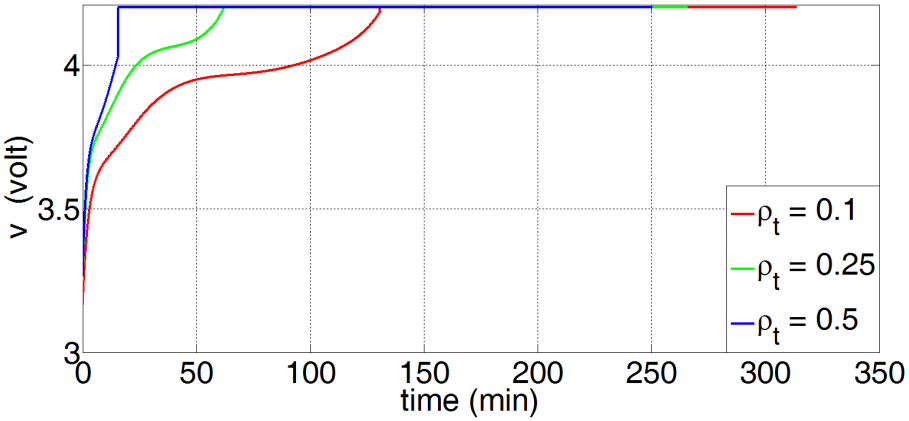

Figure 12: Terminal voltage profiles for different values of ρ_t

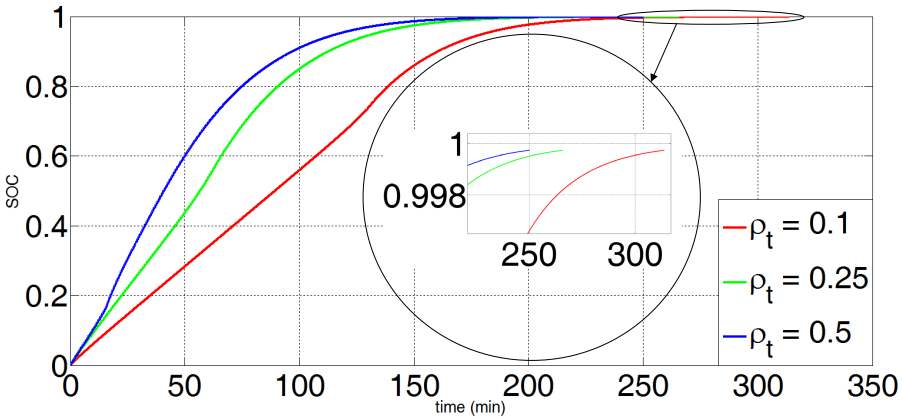

Figure 11: SOC profiles for different values of ρ_t

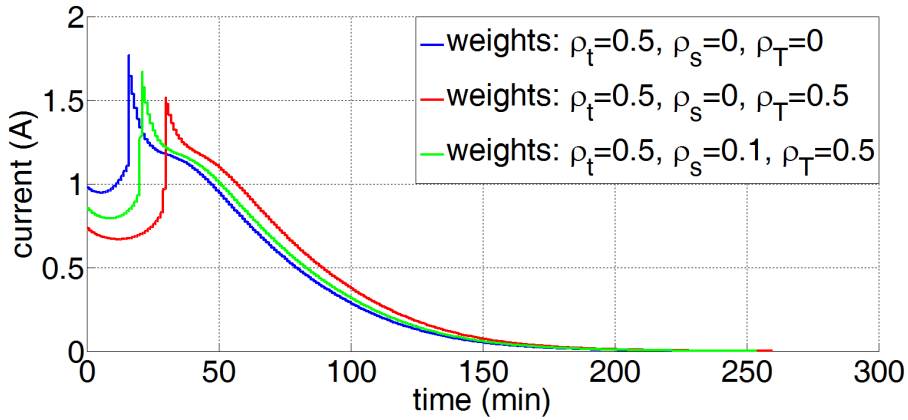

Figure 13: Current profiles for different values of ρ_T

Analysis of Different Commercial Batteries

OtE was applied to 16 commercial batteries. Sam-EB575152 (Cell 3) has the lowest efficiency (90.73%). This can be attributed to the high resistance of this battery, which might be due to aging.

Sam-EB504465 (Cell 4) has the highest TTC (102 minutes) and Nokia BP-4L (Cell 4) has the highest efficiency.

Note that the cells of the same battery type are close to each other in terms of efficiency and TTC.

Considering all the cells of the same battery type, LG-LGIP cells (circle markers) have the highest efficiency (91.4%) .

Fig. 15 shows the cost function values of $J_{\mathrm{tE}} = \rho_{\mathrm{t}} J_{\mathrm{t}} + J_{\mathrm{E}}$. When TTC is weighted with weight value of $\rho_{\mathrm{t}} = 0.5$, Sam-EB575152 (Cell 2) has the best performance.

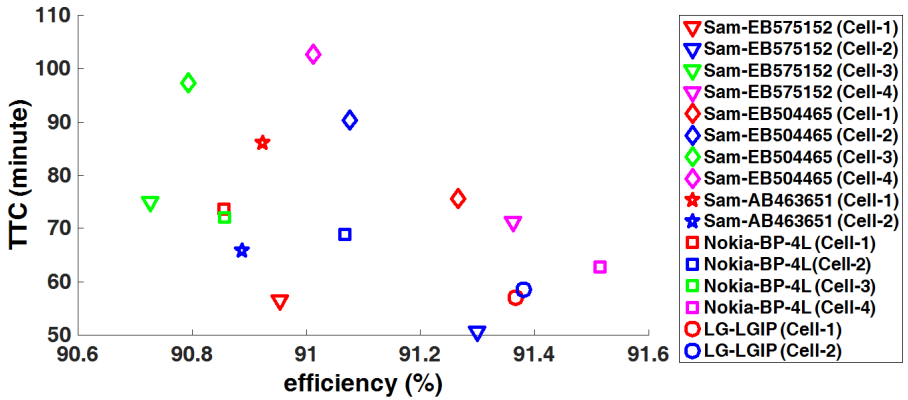

Figure 14: TTC versus Efficiency of Different Battery Types at 25°C

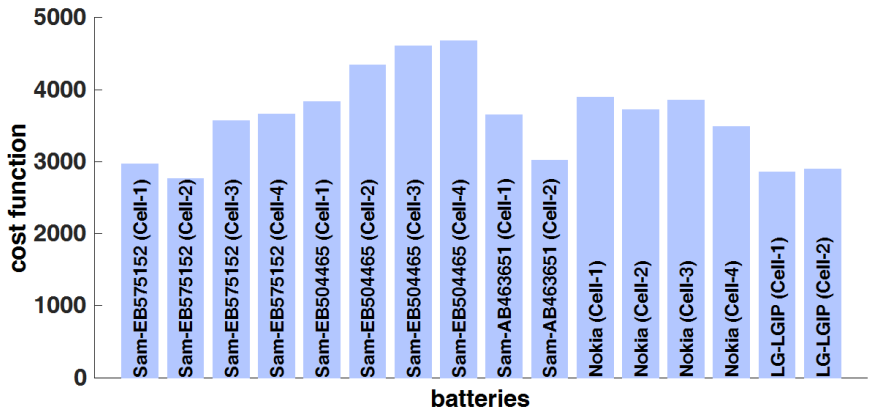

Figure 15: Cost Function for Different Battery Types at 25°C, $\rho_{\mathrm{t}} = 0.5$

Illustration of Capacity Fade

Animation 3 is based on the experimental data, obtained from 200 Charge-Rest-Discharge-Rest (CRDR) events, applied to a Samsung GS-4 battery.

As the number of cycles increases, the duration of CRDR events reduces, which is due to a decrease in the battery capacity.

Animation 3: Reduction in CRDR duration as a surrogate of capacity fade

Illustration of Power Fade

Note that Animation 3 (in the previous slide) also illustrates power fade in a battery as it ages. A jump in the current results in a jump in the terminal voltage. The series resistance of a battery (R_0) equals to the ratio of the jump in the terminal voltage to the jump in the current. If the jump in the current remains fixed, as the number of cycles increases, the change in the jump in the terminal voltage is proportional to the change in the series resistance in the battery as it ages. One can see as the current jumps from $-2.6A(-1\,\text{Crate})$ to $-130mA(-\frac{1}{20}\,\text{Crate})$, the magnitude of the jump in terminal voltage increases as the number of cycles goes up. This demonstrates that the series resistance in the battery increases as the battery ages, which demonstrates power fade in the battery due to aging.

LAR-$\alpha\beta\gamma$ Model

In order to study the effects of aging on capacity, ten different experiments were performed. The Samsung GS4 batteries, used in these experiments, have a capacity of 2600 mAh and a nominal terminal voltage of 4.35 volts.
The batteries were exposed to several (from 25 to 200) cycles of charging and discharging with a 10-minute rest after any charge or discharge process.
The following model provided good performance for tracking the trend in capacity fade.

$$Q_{\text{norm}}[n] = \alpha\beta^n n^\gamma \qquad n = 1, 2, \ldots \tag{42}$$

where n is the cycle counter and $Q_{\text{norm}}[n] = Q[n]/Q[1]$. The fitting is performed using Least Absolute Residuals (LAR) as optimization criterion.

For performance comparison with the LAR-$\alpha\beta\gamma$ model, the following bi-exponential model, which is frequently used in the literature, was chosen.

$$Q_{\text{norm}}[n] = \alpha_1\beta_1^n + \alpha_2\beta_2^n \qquad n = 1, 2, \ldots \tag{43}$$

We refer to it as LS-BE (Least Squares - Bi-Exponential).

Performance Comparison of LAR-$\alpha\beta\gamma$ and LS-BE Models

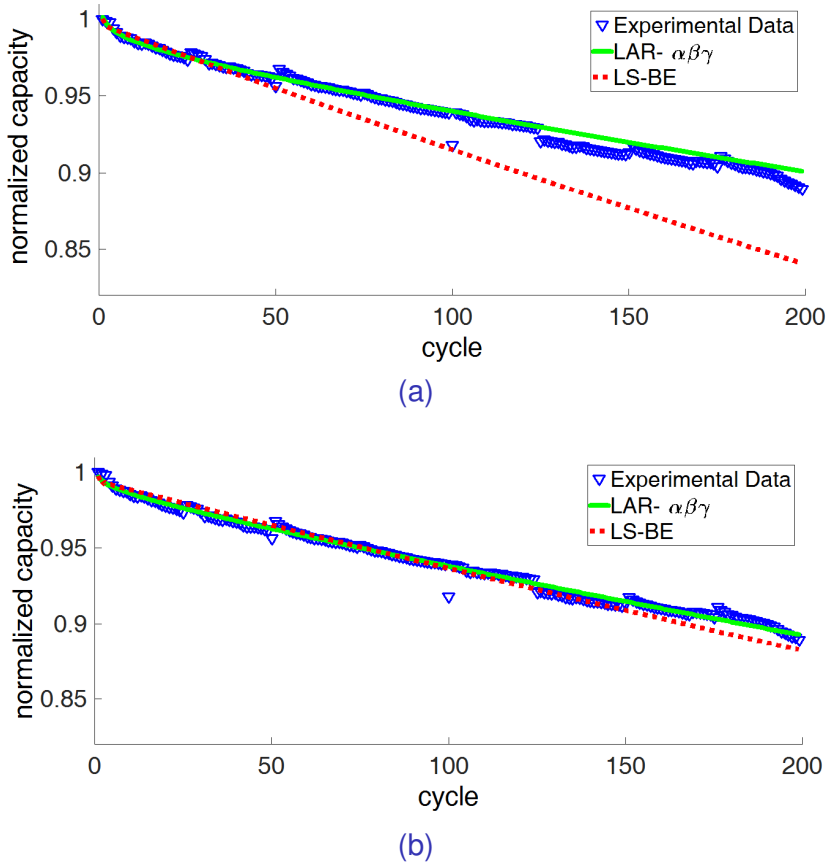

Figure 16: Comparison of LAR-$\alpha\beta\gamma$ model and LS-BE model: (a) 40 training samples (b) 160 training samples

Performance Comparison of LAR-$\alpha\beta\gamma$ and LS-BE Models

Here, we compare LAR-$\alpha\beta\gamma$ and the LS-BE models using the Akaike Information Criterion (AIC). The AIC is used to rank multiple models in the Kullback-Leibler information sense. AIC measures the goodness-of-fit and parsimony, two often-counteracting factors.

As a rule of thumb, the level of empirical support for a model with higher AIC is considerably low when the AIC difference is between 4 and 7, and it is essentially none when the AIC difference is greater than 10.

The relative likelihood of LS-BE model (with respect to LAR-$\alpha\beta\gamma$) can be calculated using the AIC differences as

$$l_{\mathrm{LS-BE}} = \exp(-\frac{\Delta\mathrm{AIC}}{2}) \tag{44}$$

Table 1: AIC differences of the LAR-$\alpha\beta\gamma$ and LS-BE models and relative likelihood of LS-BE model for all aging experiments

Experiment ID	1	2	3	4	5	6	7	8	9	10
$\Delta\mathrm{AIC} = \mathrm{AIC}_{\mathrm{LS-BE}} - \mathrm{AIC}_{\mathrm{LAR}-\alpha\beta\gamma}$	257	128	32	16	7.5	16	4.5	11	25	11
$l_{\mathrm{LS-BE}}$ (Relative likelihood)	0.00	0.00	0.00	0.00	0.02	0.00	0.10	0.00	0.00	0.00

Control Variable-Dependent (CVD) Model

To apply the level-I control policy to select the optimal values for the maximum allowable current and the maximum allowable terminal voltage, we need a capacity fade model that incorporates these two parameters. For this reason, we developed a control variable-dependent model (CVD model), in which the α, β, and γ parameters are dependent on $v_{\max}$, and $i_{\max}$. The model chosen for this purpose is as follows:

$$Q_{\text{norm},v_{\max},i_{\max}}[n] = (\alpha_1 v_{\max}^{\alpha_2} i_{\max}^{\alpha_3})\,(\beta_1 v_{\max}^{\beta_2} i_{\max}^{\beta_3})^n n^{(\gamma_1+\gamma_2 v_{\max}+\gamma_3 i_{\max})} \qquad n = 1, 2, \ldots \tag{45}$$

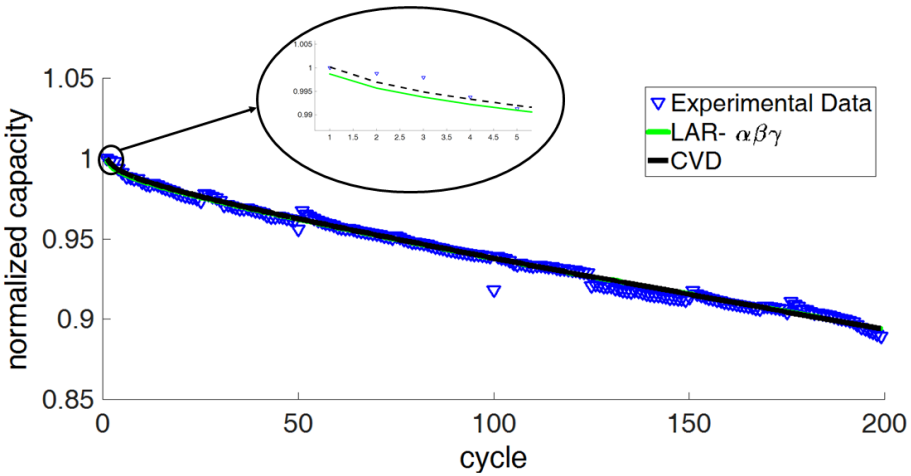

Figure 17: Comparison of CVD of LAR-$\alpha\beta\gamma$ models

Block Diagram of Battery Life Management (BLM)

The block diagram of battery life management (level-I optimization) is shown in Fig. 18. The measured capacity data from aging experiments is fed into a capacity fade model that uses the present cycle and the capacity of the battery, obtained from the battery fuel gauge (BFG), to select the optimal charging parameters $v_{\max}$ and $i_{\max}$ to be used as control parameters in the charging algorithm.

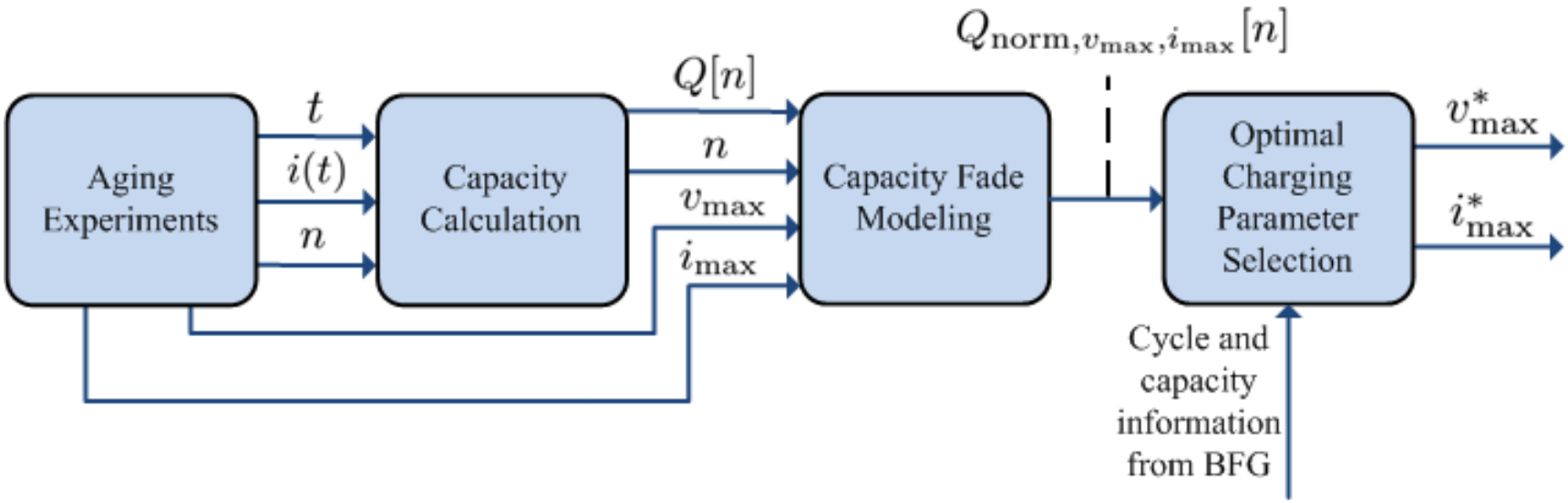

Figure 18: Block diagram of battery life management (level-I optimization)

Illustration of Expected Useful Cycle Life of Battery

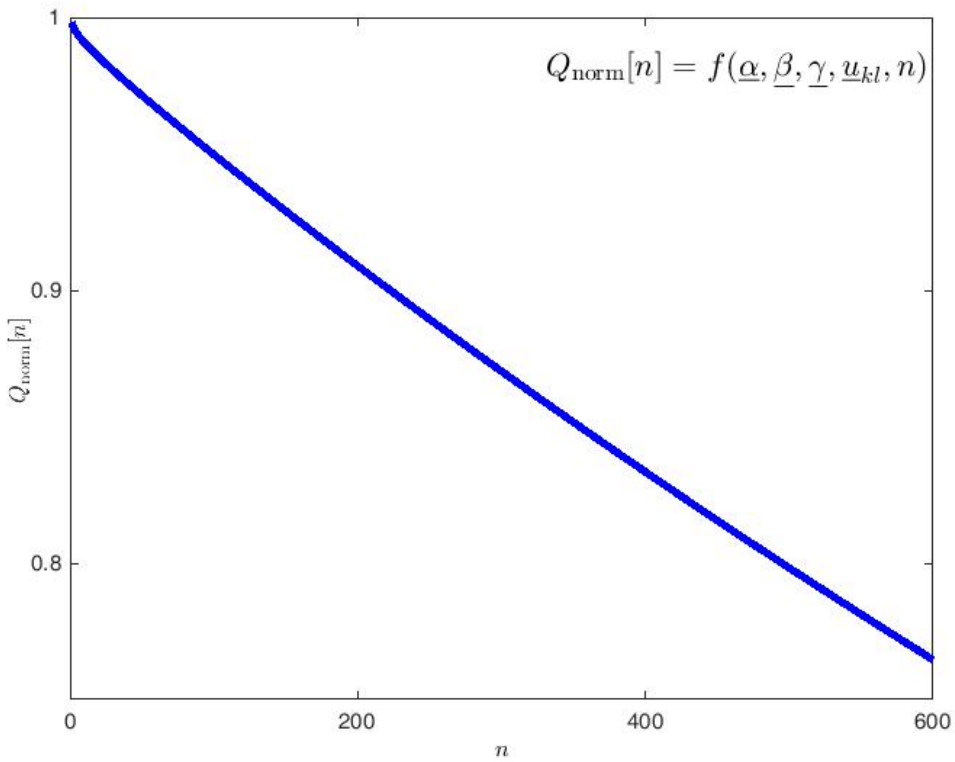

Figure 19: Illustration of BLM Algorithm

Illustration of Expected Useful Cycle Life of Battery

LPNC: Least Permissible Normalized Capacity (typically 80%)
UCL: Useful Cycle Life

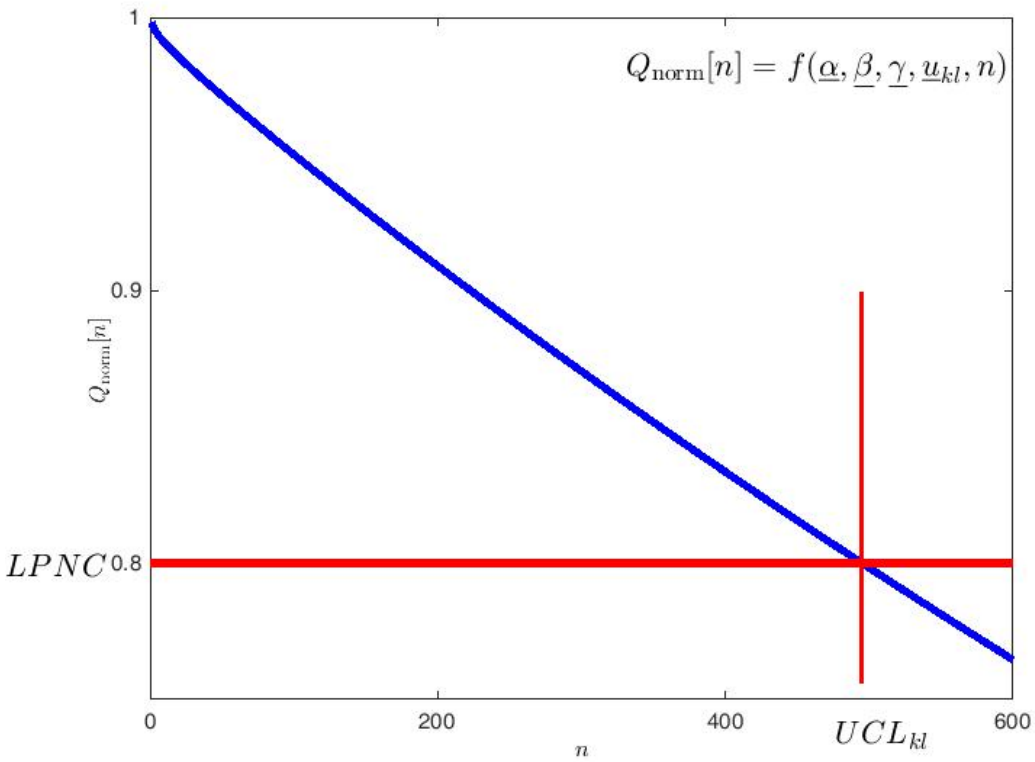

Figure 20: Illustration of BLM Algorithm

Illustration of Expected Useful Cycle Life of Battery

LPNC: Least Permissible Normalized Capacity (typically 80%)
UCL: Useful Cycle Life
PC : Present Cycle
VPC: Virtual Present Cycle

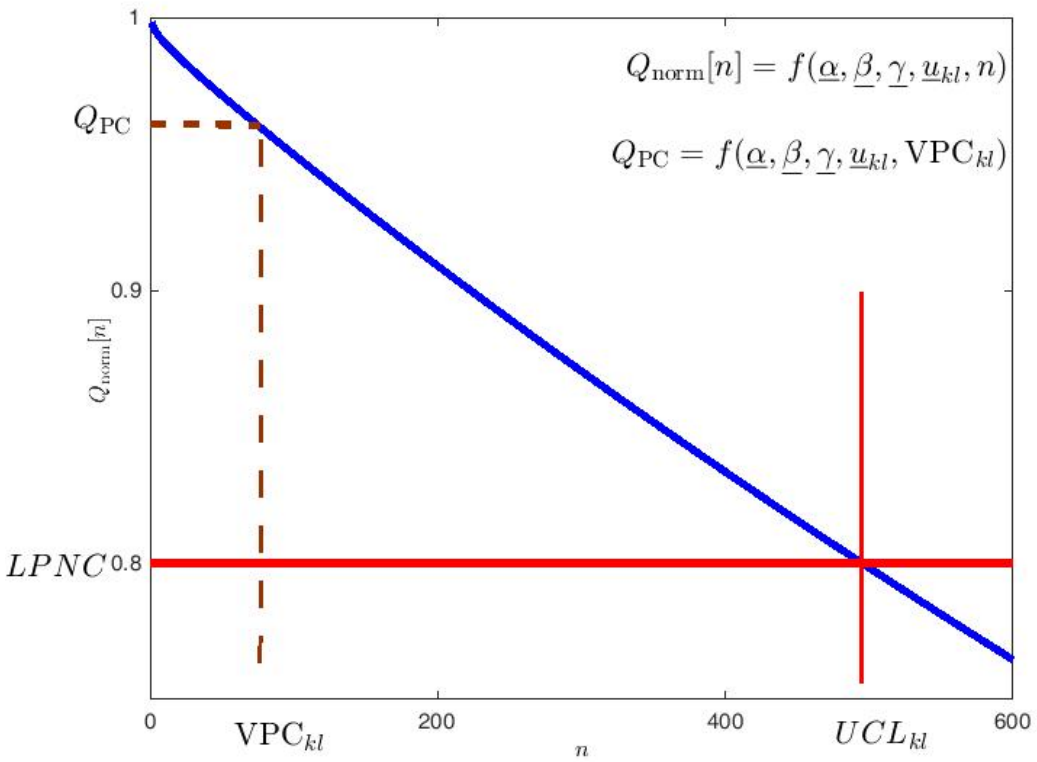

Figure 21: Illustration of BLM Algorithm

Illustration of Expected Useful Cycle Life of Battery

LPNC: Least Permissible Normalized Capacity (typically 80%)
UCL: Useful Cycle Life
PC : Present Cycle
VPC: Virtual Present Cycle
RUCL: Remaining Useful Cycle Life

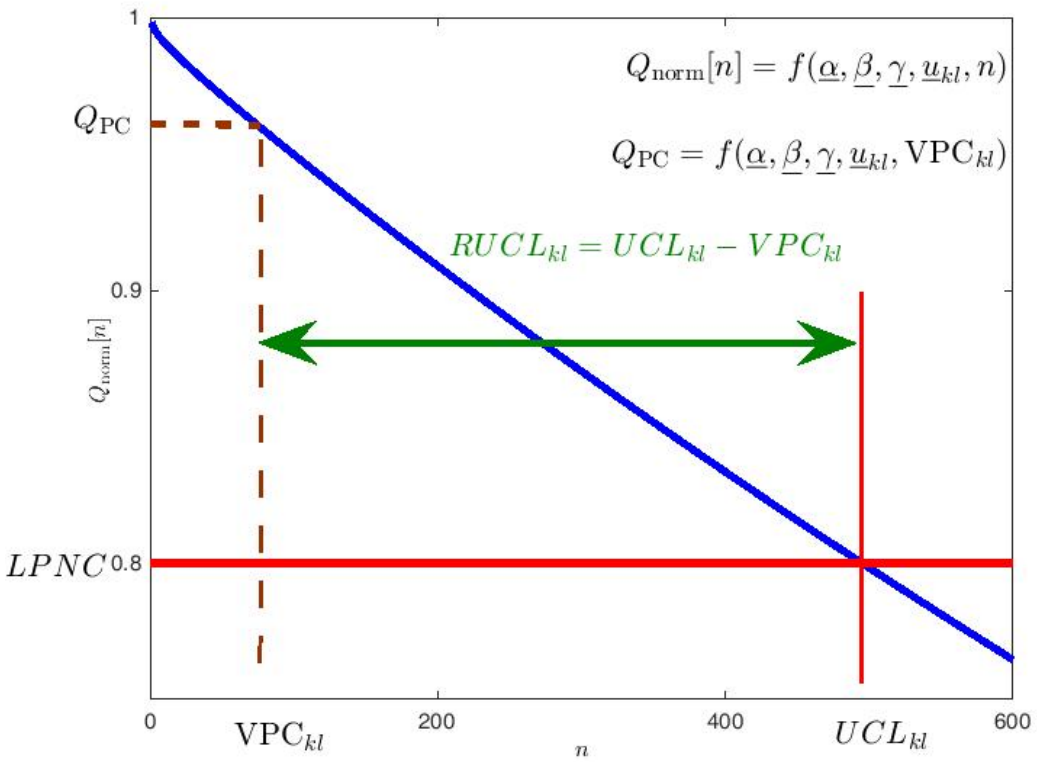

Figure 22: Illustration of BLM Algorithm

Illustration of Expected Useful Cycle Life of Battery

LPNC: Least Permissible Normalized Capacity (typically 80%)
UCL: Useful Cycle Life
PC : Present Cycle
VPC: Virtual Present Cycle
RUCL: Remaining Useful Cycle Life
EUCL: Expected Useful Cycle Life

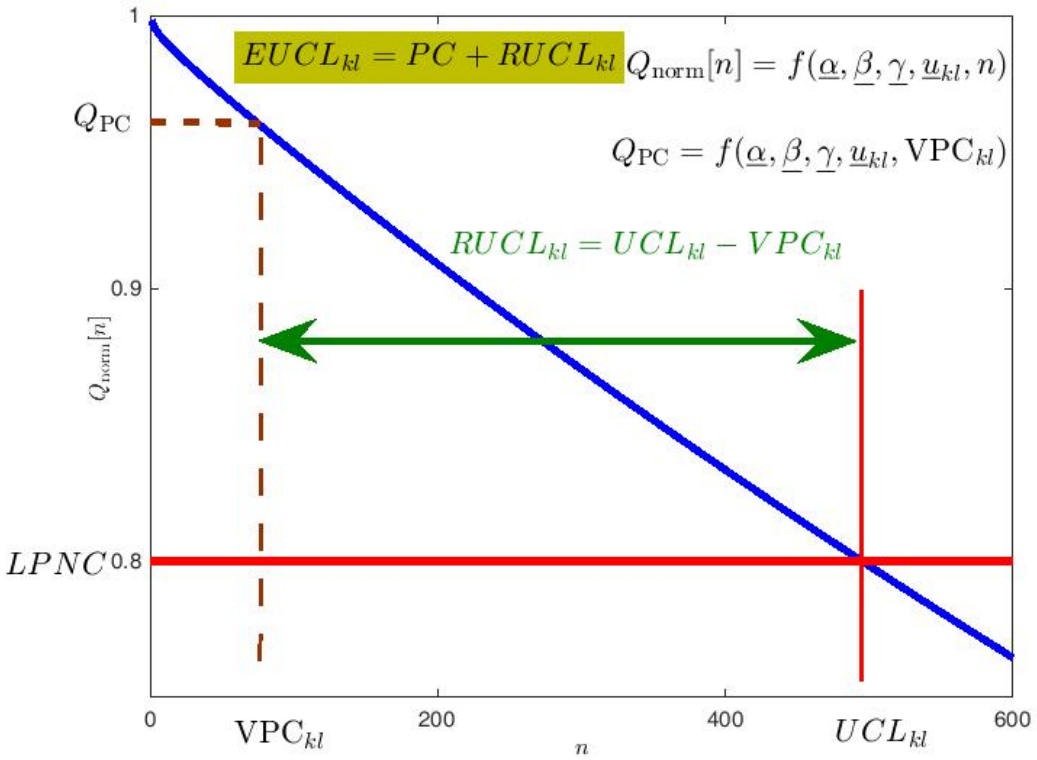

Figure 23: Illustration of BLM Algorithm

Derivation of BLM Algorithm

LPNC: Least Permissible Normalized Capacity (typically 80%)
UCL : Useful Cycle Life
PC : Present Cycle
VPC: Virtual Present Cycle
RUCL: Remaining Useful Cycle Life
EUCL: Expected Useful Cycle Life
NCL : Nominal Cycle Life
SFCS: Set of Feasible Control Settings

$$v_{\max} \in \{v_1, v_2, \ldots, v_K\} \tag{46}$$

$$i_{\max} \in \{i_1, i_2, \ldots, i_L\} \tag{47}$$

$$Q_{\text{norm},\underline{u}_{kl}}[n] = f(\underline{\alpha}, \underline{\beta}, \underline{\gamma}, \underline{u}_{kl}, n) \tag{48}$$

$$\underline{u}_{kl} = \begin{bmatrix} v_k & i_l \end{bmatrix}^T \qquad k \in \{1,2,...,K\} \qquad l \in \{1,2,...,L\} \tag{49}$$

$$\underline{\alpha} = \begin{bmatrix} \alpha_1 & \alpha_2 & \alpha_3 \end{bmatrix}^T, \ \underline{\beta} = \begin{bmatrix} \beta_1 & \beta_2 & \beta_3 \end{bmatrix}^T, \ \underline{\gamma} = \begin{bmatrix} \gamma_1 & \gamma_2 & \gamma_3 \end{bmatrix}^T \tag{50}$$

$$Q_{\text{norm},\underline{u}_{kl}}[n] = f(\underline{\alpha}, \underline{\beta}, \underline{\gamma}, \underline{u}_{kl}, n) \geq \text{LPNC} \qquad \text{for} \quad n \leq \text{UCL}_{kl} \tag{51}$$

$$Q_{\text{norm},\underline{u}_{kl}}[n] = f(\underline{\alpha}, \underline{\beta}, \underline{\gamma}, \underline{u}_{kl}, n) < \text{LPNC} \qquad \text{for} \quad n > \text{UCL}_{kl} \tag{52}$$

$$Q_{\text{PC}} = f(\underline{\alpha}, \underline{\beta}, \underline{\gamma}, \underline{u}_{kl}, \text{VPC}_{kl}) \tag{53}$$

$$\text{RUCL}_{kl} = \text{UCL}_{kl} - \text{VPC}_{kl} \tag{54}$$

$$\text{EUCL}_{kl} = \text{PC} + \text{RUCL}_{kl} \tag{55}$$

$$\text{EUCL}_{kl} = (\text{PC} - \text{VPC}_{kl}) + \text{UCL}_{kl} \tag{56}$$

$$\text{EUCL}_{kl} \geq \text{NCL} \tag{57}$$

$$\text{SFCS} = \{\underline{u}_{kl} | k \in \{1,2,...,K\}, l \in \{1,2,...,L\}, \text{EUCL}_{kl} \geq \text{NCL}\} \tag{58}$$

$$(k^*, l^*) = \arg \left(\min_{\underline{u}_{kl} \in \text{SFCS}} (\text{TTC}_{kl}) \right) \tag{59}$$

$$\underline{u}^* = \begin{bmatrix} v^*_{\max} & i^*_{\max} \end{bmatrix}^T = \begin{bmatrix} v_{k^*} & i_{l^*} \end{bmatrix}^T \tag{60}$$

Battery Life Management Block Diagram

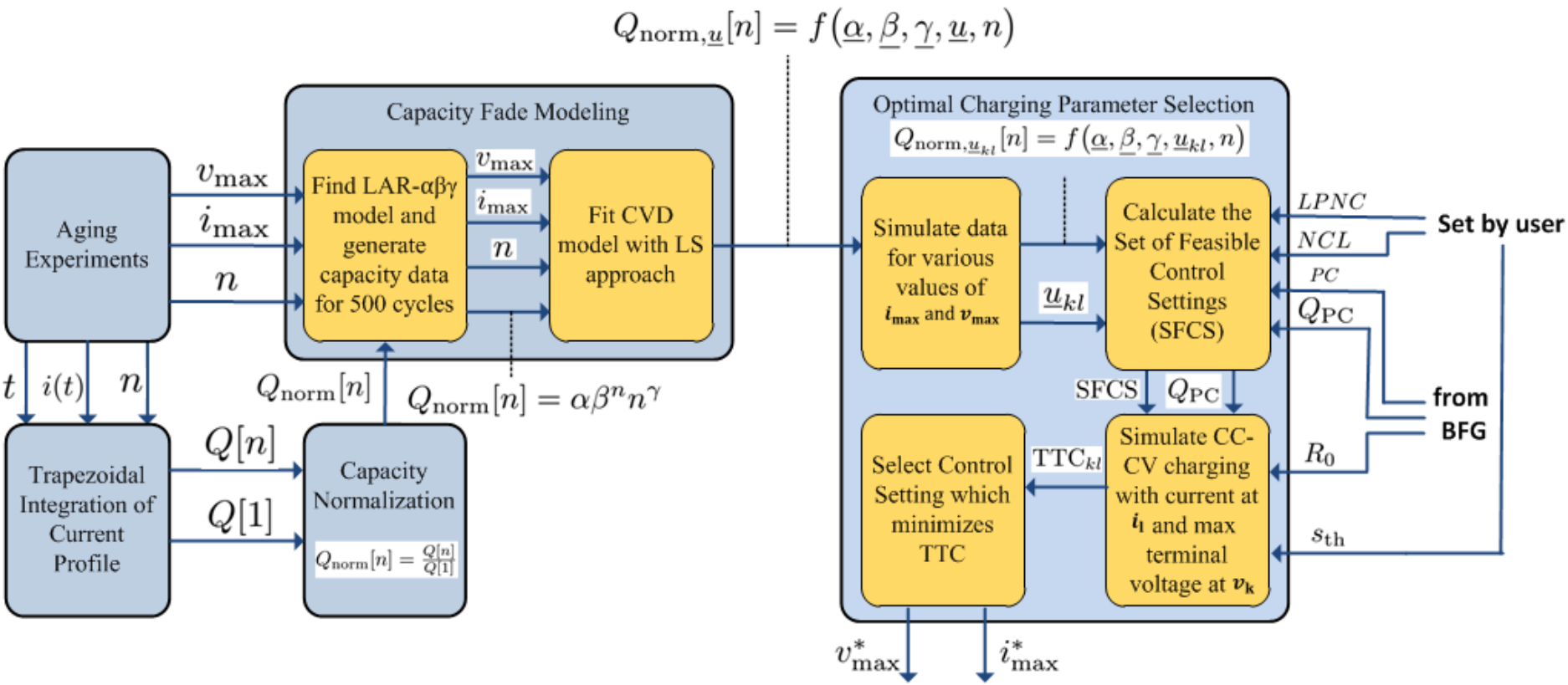

Figure 24: Battery life management block diagram

Numerical Illustration of Optimal Charging Parameter Selection

Table 2: Expected Useful Cycle Life (EUCL), for $PC = 50$, $Q_{\text{PC}} = 0.96$, $R_0 = 150\,m\Omega$, and $s_{\text{th}} = 0.80$

v_k \ i_l	0.7 (1.82)	0.8 (2.08)	0.9 (2.34)	1.0 (2.6)	1.1 (2.86)	1.2 (3.12)	1.3 (3.38)
0.97 (4.22)	**590**	**568**	**550**	**536**	**523**	**512**	**502**
0.98 (4.26)	**567**	**547**	**531**	**517**	**505**	494	485
0.99 (4.31)	**546**	**527**	**512**	498	488	478	469
1.00 (4.35)	**526**	**508**	495	482	472	462	454
1.01 (4.39)	**507**	491	477	466	456	448	440
1.02 (4.44)	489	474	461	450	442	433	426

EUCL, Capacity Fade and Optimal Strategy

Battery is exposed to 50 cycles.
Normalized capacity of the battery at the present cycle changing from 0.99 to 0.96.
Corresponding EUCL values reduce.
Infeasible strategies are shown in red.
The optimal strategy is shown in green.

Remark

As the battery capacity reduces, lower values of $v_{\max}$ become optimal.

Animation 4: Effect of capacity fade on optimal strategy

EUCL, Power Fade and Optimal Strategy

Battery is exposed to 50 cycles.
The resistance of the battery is increased from $150\,m\Omega$ to $300\,m\Omega$.
Corresponding EUCL values do not change.
Infeasible strategies are shown in red.
The optimal strategy is shown in green.

Remark

As the battery power fades (the resistance increases), lower values of $i_{\max}$ become optimal.

Animation 5: Effect of power fade on optimal strategy

Tripartite Digraph for Fault Diagnosis

Fault diagnosis system can be conceptualized as a tripartite directed graph (digraph) as shown in Fig. 25.

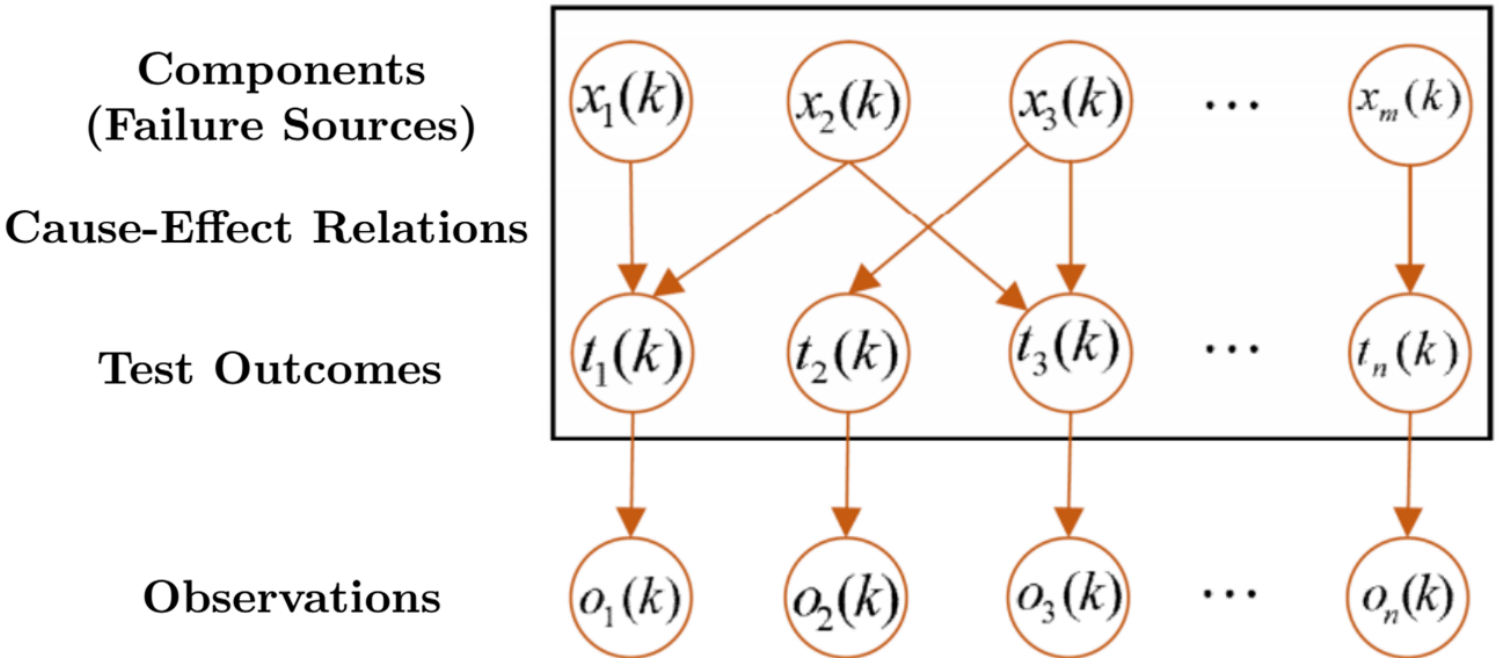

Figure 25: Tripartite digraph of fault diagnosis system

Modeling Abstraction in Fault Diagnosis

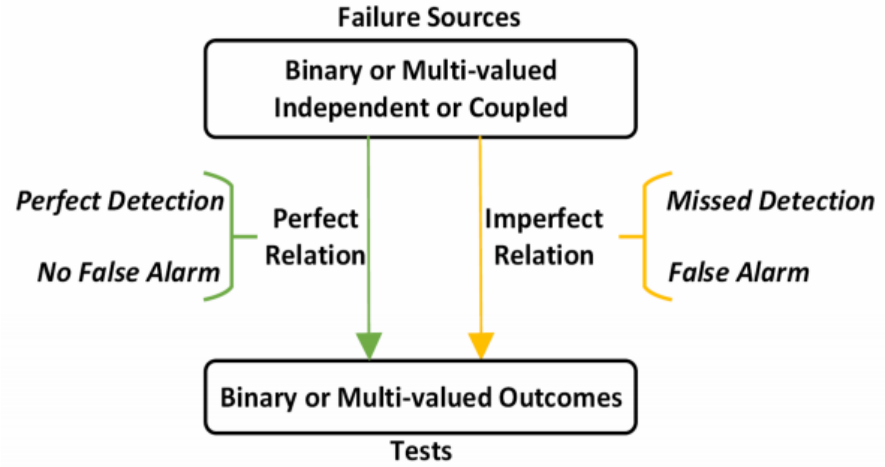

Figure 26: Modeling abstractions in fault diagnosis subsystems

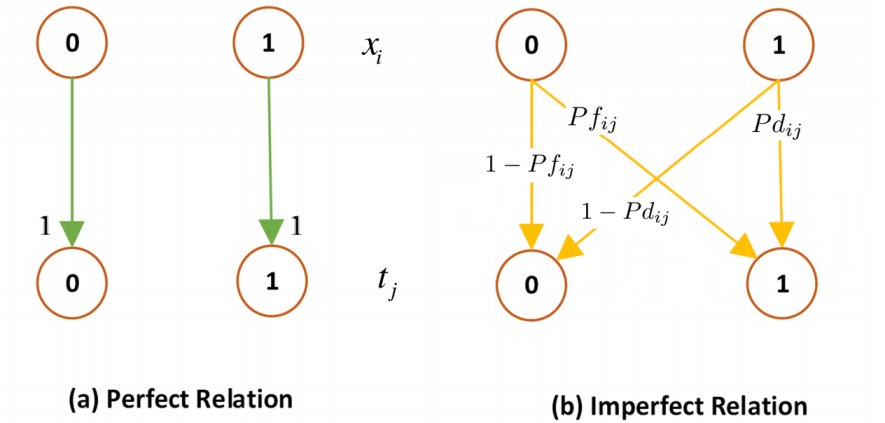

Figure 27: Perfect and imperfect relations of a failure source and a test outcome

Static Multiple Fault Diagnosis (SMFD)

Static Multiple Fault Diagnosis (SMFD) Problem

Given T, a subset of all test outcomes, what are the most likely states of failure sources, $\mathbf{x}$?
Formally:

$$\hat{\mathbf{x}} = \arg \max_{\mathbf{x}} \Pr(\mathbf{x}|T) \tag{61}$$

Equation (61) can be written as (using Bayes' rule):

$$\hat{\mathbf{x}} = \arg \max_{\mathbf{x}} \ln(\Pr(T|\mathbf{x}) \Pr(\mathbf{x})) \tag{62}$$

$$\hat{\mathbf{x}} = \arg \max_{\mathbf{x}} \left\{ \ln\left(\Pr\left(T_f|\mathbf{x}\right)\right) + \ln(\Pr(T_p|\mathbf{x})) + \ln(\Pr(\mathbf{x})) \right\} \tag{63}$$

Static Multiple Fault Diagnosis (SMFD)

The cost function can be written as follows:

$$J(\mathbf{x},\mathbf{y}) = \sum_{t_j \in T_f} \ln(1-y_j) + \sum_{t_j \in T_p} \sum_{i=1}^{m} \beta_{ij} x_i + \sum_{i=1}^{m} \ln(p_i) x_i. \tag{64}$$

where

$$\beta_{ij} = \ln\left(\frac{\overline{Pd_{ij}}}{\overline{Pf_{ij}}}\right) \tag{65}$$

$$h_j = \sum_{i=1}^{m} \ln\left(\overline{Pf_{ij}}\right) \tag{66}$$

$$p_i = \frac{p_{s_i}}{1-p_{s_i}}, \quad \Pr(x_i = 1) = p_{s_i} \tag{67}$$

$$y_j = \Pr(t_j = \text{pass} | \mathbf{x}) \tag{68}$$

By defining $\alpha_i = \ln(p_i) + \sum_{t_j \in T_p} \beta_{ij}$, $c_i(\lambda) = \alpha_i - \sum_{t_j \in T_f} \lambda_j \beta_{ij}$, the relaxed objective function will be as follows:

$$L(\mathbf{x},\mathbf{y},\lambda) = \sum_{t_j \in T_f} \{\ln(1-y_j) + \lambda_j \ln(y_j) - h_j \lambda_j\} + \sum_{i=1}^{m} c_i(\lambda) x_i. \tag{69}$$

Some Insights from SMFD Problem Formulation

Insight 1

If tests are perfect, for any passed test t_j, i.e., $t_j \in T_p$, the set of all components that are associated with test t_j should be healthy.

The above insight substantially reduces the cardinality of failure sources, S, by discarding the failure sources covered by passed tests.

Insight 2

If tests are perfect, for any failed test t_j, i.e., $t_j \in T_f$, among all components associated with the failed test, i.e. $Pd_{ij} > 0$, at least one should be faulty.

Insight 3

For any $t_j \in T_f$, we have $\lambda_j^* \leq \lambda_j^{\max}$, where $\lambda_j^{\max} = \frac{e^{h_j}}{1-e^{h_j}}$.

Insight 4

For any failure source x_i, if we have $\ln(p_i) + \sum_{t_j \in T_p} \beta_{ij} < \sum_{t_j \in T_f} \frac{\beta_{ij} e^{h_j}}{1-e^{h_j}}$, then $x_i^* = 0$.

Detection-False Alarm (DFA) and Leaky Noisy OR (LNOR) Test Models

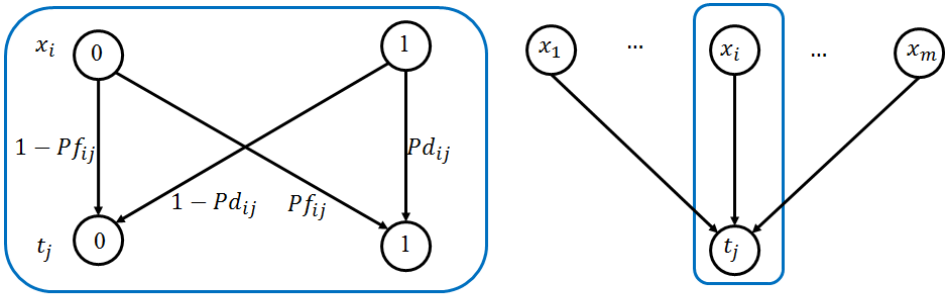

Figure 28: Detection-False Alarm (DFA) test model

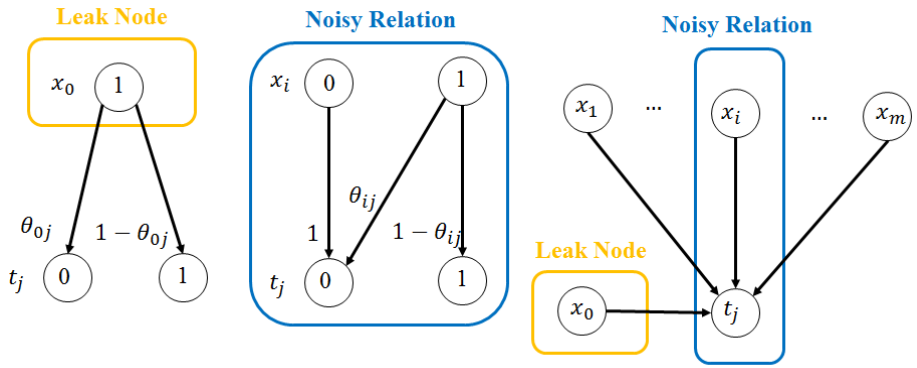

Figure 29: Leaky Noisy OR (LNOR) test model

Equivalence of DFA and LNOR Test Models

Proposition

For a DFA test model with m failure sources and n tests, and with detection probabilities $\{Pd_{ij}\}$ and false alarm probabilities $\{Pf_{ij}\}$, there exists a unique LNOR test model with the following parameters:

$$\theta_{0j} = \prod_{i=1}^{m} (1 - Pf_{ij}), \tag{70}$$

$$\theta_{ij} = \frac{1 - Pd_{ij}}{1 - Pf_{ij}}, \quad i = 1, 2, \ldots, m. \tag{71}$$

Proof: The following relation proves the existence of a unique LNOR test model for each DFA test model.

$$\begin{aligned} \Pr\{t_j = 0 | \mathbf{x}\} &= \prod_{i=1}^{m} (1 - Pf_{ij})^{1-x_i} (1 - Pd_{ij})^{x_i} \\ &= \prod_{i=1}^{m} (1 - Pf_{ij}) \left(\frac{1 - Pd_{ij}}{1 - Pf_{ij}}\right)^{x_i} \\ &= \left(\prod_{i=1}^{m} (1 - Pf_{ij})\right) \prod_{i=1}^{m} \left(\frac{1 - Pd_{ij}}{1 - Pf_{ij}}\right)^{x_i} = \theta_{0j} \prod_{i=1}^{m} \theta_{ij}^{x_i}. \end{aligned} \tag{72}$$

Logistic Regression (LR) Test Model and the Unified Test Model

The general formulation for pass outcome for LR test model is:

$$\Pr(t_j = 0|\mathbf{x}) = \frac{\exp\left(\xi_{0j} + \sum_{i=1}^{m} \xi_{ij} x_i\right)}{1 + \exp\left(\xi_{0j} + \sum_{i=1}^{m} \xi_{ij} x_i\right)} \tag{73}$$

Define (for the LR test model):

$$\theta_{0j} = \exp(\xi_{0j}), \quad \theta_{ij} = \exp(\xi_{ij}), \ i = 1, \ldots, m \tag{74}$$

Then, we can unify the LR and LNOR test models as follows:

$$z_j(\mathbf{x}) = \theta_{0j} \prod_{i=1}^{m} \theta_{ij}^{x_i}, \text{ or equivalently, } \ln(z_j(\mathbf{x})) = \beta_{0j} + \sum_{i=1}^{m} \beta_{ij} x_i \tag{75}$$

$$z_j(\mathbf{x}) = \Pr(t_j = 0|\mathbf{x}) \left(1 - \Pr(t_j = 0|\mathbf{x})\right)^{-d}, \quad d = \begin{cases} 0 & \text{Leaky Noisy OR} \\ 1 & \text{Logistic Regression} \end{cases} \tag{76}$$

Dual Cost Function for MAP inference for the Unified Test Model

The dual cost function is:

$$L(\lambda) = \sum_{t_j \in T_z} L_{1j}(\lambda_j) + \sum_{i=1}^{m} L_{2i}(\lambda) \tag{77}$$

$$\begin{aligned} L_{1j}(\lambda_j) = {} & \lambda_j \ln(\lambda_j) + (1 - d\lambda_j)\ln(1 - d\lambda_j) \\ & - (1 + (1-d)\lambda_j)\ln(1 + (1-d)\lambda_j) - \beta_{0j}\lambda_j \end{aligned} \tag{78}$$

$$L_{2i}(\lambda) = c_i(\lambda) u(c_i(\lambda)) = \max(0,\ c_i(\lambda)) \tag{79}$$

$$T_z = \begin{cases} T_f & \text{Leaky Noisy OR} \\ \\ T & \text{Logistic Regression} \end{cases} \tag{80}$$

$$c_i(\lambda) = \alpha_i - \sum_{t_j \in T_z} \lambda_j \beta_{ij}, \quad \alpha_i = \gamma_i + \beta_i, \quad i = 1, \ldots, m \tag{81}$$

$$\gamma_0 = \sum_{i=1}^{m} \ln(1 - p_{s_i}), \quad \gamma_i = \ln\left(\frac{p_{s_i}}{1 - p_{s_i}}\right), \quad \beta_i = \sum_{t_j \in T_p} \beta_{ij}, \quad i = 0, 1, \ldots, m \tag{82}$$

Some Insights

Figure 30 shows $\Pr(T = 11|\mathbf{x})\Pr(\mathbf{x})$ when there are two tests (both failed) and three failure sources. The data is generated from a weighted sum of an affine function in log-probability and an affine one in log-odds. Using any of the test models, $\mathbf{x} = 010$ has the highest probability, but the LR test model provides more robust results.

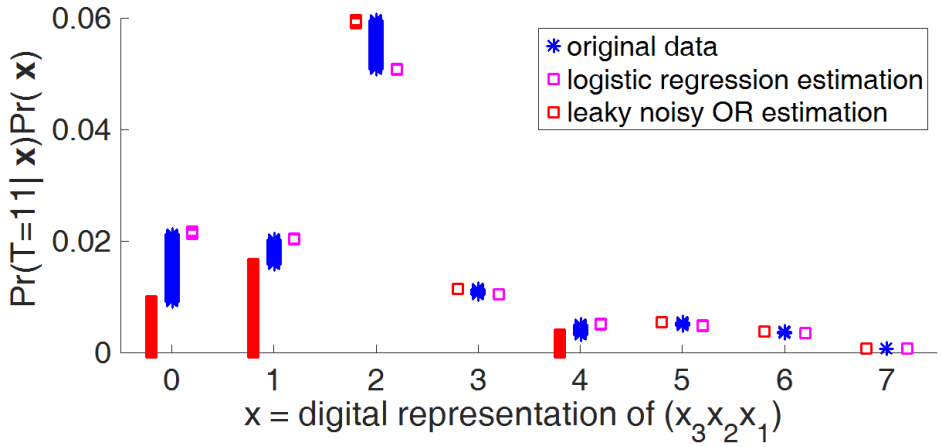

Figure 30: Comparison of $\Pr(T = 11|\mathbf{x})\Pr(\mathbf{x})$ for the LNOR and the LR test models

1. The LNOR test model is affine in log-probability, while the LR test model is affine in log-odds.
2. The LR test model provides robust performance, as the structure of observed data varies from an affine function in log-probability to an affine one in log-odds.
3. The dimension of dual cost function of LNOR test model equals the number of failed tests, while that of LR test model is independent of failed tests and is always equal to the number of all tests.

Conclusion

The primary contributions of this thesis are:

1. Derived a closed form solution for the optimal battery charging profile to minimize a weighted sum of time-to-charge and energy loss.
2. Proved that for the OCV-Resistance battery model, CC-CV is the optimal solution with respect to the objective function composed of a linear combination of time-to-charge and energy-loss.
3. Derived a semi-closed form solution for the optimal battery charging profile by adding the temperature rise index to the cost function.
4. Showed that the effect of temperature rise can be approximated as an equivalent heating resistance.
5. Derived the optimal battery charging profile for general equivalent electrical circuit models as a linear quadratic - constant voltage (LQ-CV) strategy.
6. Derived two new battery capacity fade models that are shown to be statistically superior to the bi-exponential capacity fade model.
7. Developed an optimal charging parameter selection method for selecting the best settings for the control variables to achieve a desired “useful cycle life”, while attaining the fastest possible time-to-charge.
8. Proved the equivalence of the Detection-False Alarm (DFA) and the Leaky Noisy OR (LNOR) test models.
9. Proposed a unified test model to include both the LNOR and the logistic regression (LR) test models.
10. Solved the maximum *a posteriori* (MAP) inference problem associated with the unified test model.
11. Derived a dual cost function for the fault diagnosis problem both with the DFA test model and with the unified test model.
12. Developed an algorithm for fault prognosis in systems using the unified test model.

Acknowledgment

Major advisor: Prof. Krishna R. Pattipati
Co-advisor: Prof. Yaakov Bar-Shalom
Committee member: Prof. Shengli Zhou
Support from Fairchild Semiconductor, NSF, UTC Chair Professorship and UCONN's Academic Plan is gratefully acknowledged.
Cyberlab colleagues (especially, Xu Han and Niranjan Raghunathan)
Michael Rauth, Bob Card, and Travis Williams from Fairchild Semiconductor
Department Head: Prof. Rajeev Bansal
Department Associate Head: Prof. John Chandy
Administrative Staff of the Department
My family members (especially, my mother and my wife)